

# Discrimination of the enantiomers of biphenylic derivatives in micellar aggregates formed by chiral amidic surfactants

Alessandro Alzalamira,<sup>a</sup> Francesca Ceccacci,<sup>a</sup> Donato Monti,<sup>b</sup> Stefano Levi Mortera,<sup>c</sup> Giovanna Mancini,<sup>d,e,\*</sup> Alessandro Sorrenti,<sup>a</sup> Mariano Venanzi<sup>b</sup> and Claudio Villani<sup>c</sup>

<sup>a</sup>Dipartimento di Chimica, Università degli Studi di Roma 'La Sapienza', P. le A. Moro 5, 00185 Roma, Italy

<sup>b</sup>Dipartimento di Scienze e Tecnologie Chimiche, Università degli Studi di Roma 'Tor Vergata',

Via Della Ricerca Scientifica 1, 00133 Roma, Italy

<sup>c</sup>Dipartimento di Studi di Chimica e Tecnologia delle Sostanze Biologicamente Attive, Università Degli Studi di Roma 'La Sapienza', P. le A. Moro 5, 00185 Roma, Italy

<sup>d</sup>CNR, Istituto di Metodologie Chimiche, Dipartimento di Chimica 'La Sapienza', P. le A. Moro 5, 00185 Roma, Italy

<sup>e</sup>Centro di Eccellenza Materiali Innovativi Nanostrutturati per Applicazioni Chimiche Fisiche e Biomediche, Via Elce di Sotto, 06123 Perugia, Italy

Received 5 July 2007; accepted 30 July 2007

**Abstract**—The chirality of micellar aggregates formed by surfactants derived from L-proline was investigated by using two chiral biphenylic derivatives as probes of chirality. The investigation carried out by <sup>1</sup>H NMR, circular dichroism, and HPLC on chiral phase demonstrates that chiral recognition may occur in sites of the aggregates far from the head-group stereogenic centers and it is due to interaction with a whole region of the aggregate rather than with a single monomer in the aggregate. Subtle changes of the structure of the monomer influence the aggregation properties of the surfactants and its expression of chirality.

© 2007 Elsevier Ltd. All rights reserved.

## 1. Introduction

Many systems in Nature are chiral and lack their mirror image. This parity violation is observed at different levels of complexity, from subatomic particles, atoms, and molecules to the macroscopic level of some plants and animals.

Several investigations suggest that the chiral homogeneity of biomolecules might reflect the chirality of electroweak forces;<sup>1</sup> considering systems of higher complexity, it is known that the chiral homogeneity of biomolecules, such as sugars and amino acids, affects the chirality of DNA and proteins. However, the transfer of the chiral information from the molecular level to the macroscopic levels, at length scales of nanometers, centimeters, and higher and at high levels of complexity is not completely understood, although numerous investigations have dealt with

this topic and some transfer mechanisms have been elucidated.<sup>2</sup>

Chiral and enantiopure lipids and proteins self-assemble and organize, according to their molecular structure, to form cell membranes; this process brings into being a large number of complex functions that are responsible for cell life processes. Chirality, as part of the molecular structure, influences the organization and functions of the lipid double layer; however, its role is still poorly understood. It is unclear how the chiral information is translated from the monomers to the assembly, how and where the membrane system expresses the chiral function. Since cell membranes are composed of hundreds of different components, the investigations on these complex systems have been carried out on models such as micelles or liposomes.<sup>3</sup>

We have largely investigated chiral recognition in micellar aggregates formed by sodium *N*-dodecanoyl-L-prolinate **1** by using, as probes of chirality, either the enantiomers of dipeptides<sup>3i</sup> or the racemic mixtures of biphenylic derivatives.<sup>3e,l,p</sup> The modulation of the molecular structure of

\* Corresponding author. Tel.: +39 0649913078; fax: +39 06490421; e-mail: [giovanna.mancini@uniroma1.it](mailto:giovanna.mancini@uniroma1.it)

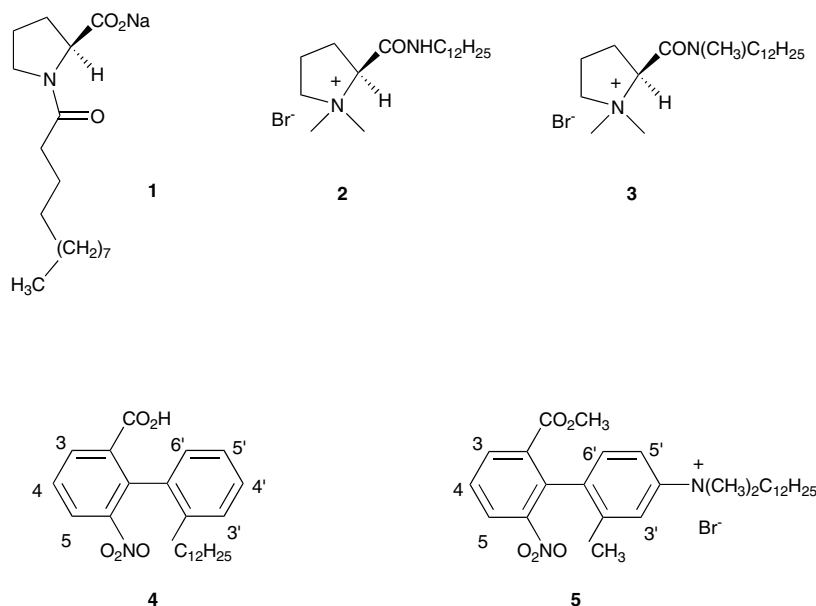
the probe allowed us to evidence some sites of chiral recognition in the micellar aggregates.

Herein, we take into consideration two other amidic surfactants, obtained from L-proline, where the head groups are positively charged and the amide function involves the proline carboxylic group and a primary or a secondary hydrophobic amine, namely (2*S*)-*N*-dodecyl-1,1-dimethylpyrrolidinium-2-carboxamide bromide **2** and (2*S*)-*N*-dodecyl-*N*,1,1-trimethylpyrrolidinium-2-carboxamide bromide **3**.

The investigations were carried out by circular dichroism (CD), HPLC, and  $^1\text{H}$  NMR by using as probes of the chirality of the micellar aggregates two biphenylic derivatives, 2-carboxy-2'-dodecyloxy-6-nitrobiphenyl **4** and *N,N*-dimethyl-*N*-dodecyl-*N*-[4-(2'-methoxycarbonyl-6'-nitrophenyl)-3-methoxy]-phenylammonium bromide **5**. Both biphenylic derivatives were previously used for investigating the chirality of the aggregates formed by **1**, since the different positions of the hydrophobic chain on the aromatic system imposes a different orientation of the biphenylic system inside the aggregates, allowing the exploration of different regions of the aggregates.

were measured by conductivity measurements at 298 K and are  $3.72 \pm 0.05$  mM and  $4.42 \pm 0.11$  mM for **2** and **3**, respectively. Aggregation numbers of aggregates obtained at 40.0 mM (75 and 51 for **2** and **3**, respectively) and 100.0 mM (87 and 66 for **2** and **3**, respectively) were measured by a time-resolved fluorescence quenching technique, based on pyrene/cetylpyridinium chloride as a fluorophore–quencher pair.<sup>4</sup>

The  $^1\text{H}$  NMR spectra of 40 mM aqueous solutions of surfactants (Fig. 1) show the presence of the isomers relative to the amidic bond in 100:1 and 2:1 ratios for **2** and **3**, respectively (M and m will be used for indicating the major and minor isomer, respectively). The  $^{13}\text{C}$  NMR spectrum of the 40 mM aqueous solution of **3** shows the split of signals, due to terminal methyl of the alkyl chain (Fig. 2), demonstrating the organization in domains, according to the stereochemical information, as previously observed for other amidic surfactants.<sup>5</sup> In the case of **2**, the presence of the minor isomer is only detectable in the  $^1\text{H}$  NMR spectrum. The larger line width of signals due to **2** with respect to signals due to **3** is in agreement with the higher aggregation number found for aggregates of **2** with respect to aggregates of **3**.



## 2. Results and discussion

### 2.1. Preparation and characterization of surfactants

Surfactants **2** and **3** were prepared by quaternization, using CH<sub>3</sub>Br, of the corresponding amines, obtained by the reaction of *N*-methyl-L-proline with 1-aminododecane and *N*-methyl-1-aminododecane, respectively, in the presence of EDCHCl and HOBT.

Both surfactants are soluble in water at 40.0 mM concentration at 277 K; therefore, their Krafft temperature at 40.0 mM and their Krafft point are below 277 K. CMCs

### 2.2. Chiral recognition experiments on biphenylic derivative **4**

The rotational barrier of biphenylic derivative **4** is such ( $\sim 22$  kcal/mol)<sup>6</sup> that the transfer of chiral information from the aggregates to the probe may very easily induce an imbalance in its enantiomer equilibrium (deracemization) that may be detected by NMR, CD, and HPLC.<sup>7</sup>

In Figure 3, we report the aromatic region of the  $^1\text{H}$  NMR spectra of a 4.0 mM **4** in 40.0 mM aqueous **2** (Fig. 3a) and in 40.0 mM aqueous **3** (Fig. 3b).

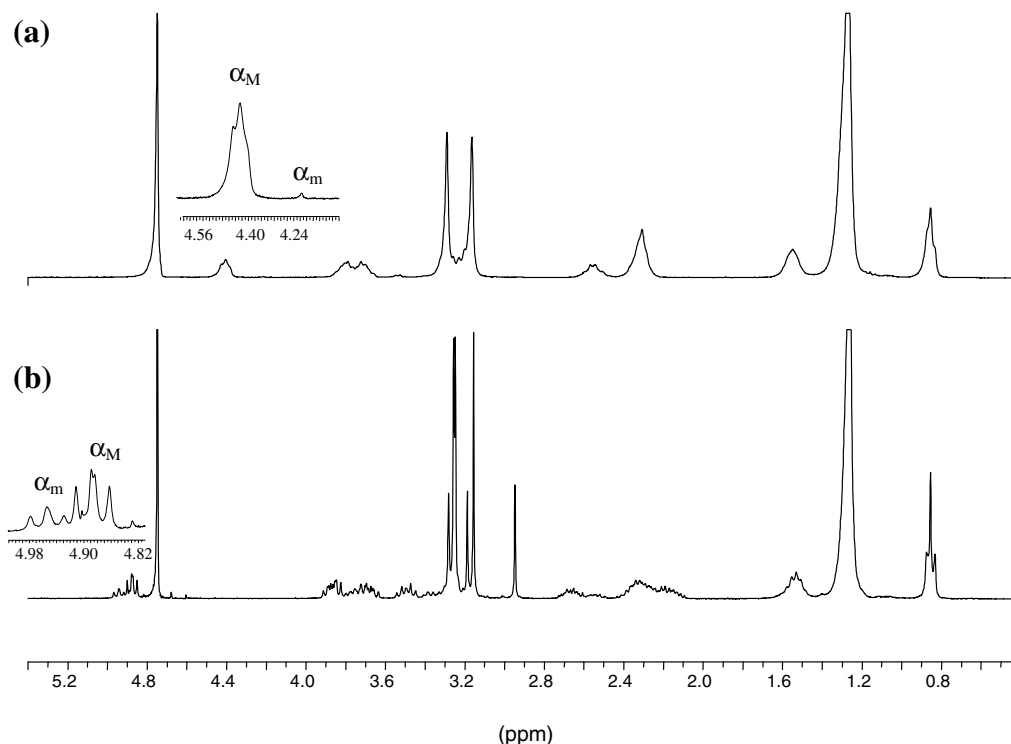


**Figure 1.**  $^1\text{H}$  NMR spectrum of an aqueous 40.0 mM solution of (a) surfactant **2**, (b) surfactant **3**. Insets show signals due to the  $\alpha$  protons of amidic isomers ( $\alpha_M$  and  $\alpha_m$ , major and minor isomer, respectively).

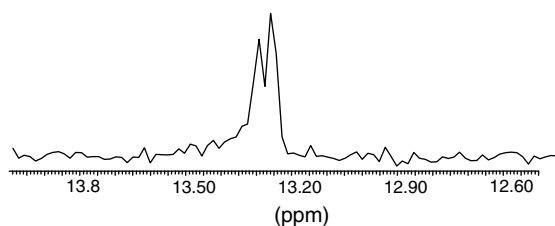


**Figure 2.** Region of the  $^{13}\text{C}$  NMR spectrum of aqueous 40.0 mM **3** relative to signals due to the terminal methyl of the amidic isomers.

The spectrum reported in Figure 3a shows the presence of two patterns of signals characterized by different intensities. These signals could be due to the diastereomeric interactions of the enantiomers of **4** with the chiral aggregates, and therefore they would be the result of a high extent of deracemization, given the large difference in intensity observed. Alternatively, they could be due to the specific interactions of **4** with the isomers of the surfactant. The  $^1\text{H}$  NMR spectrum relative to 4.0 mM **4** in 40.0 mM aqueous **3** (Fig. 3b) shows a single pattern of signals.

The CD spectra of biphenylic derivative **4** in the aqueous solutions of surfactants **2** and **3** show a negative CD band centered at 330 nm (Figs. 4 and 5). The corresponding surfactant aqueous solutions in the absence of **4** and the corresponding methanol solutions containing surfactant and biphenylic derivative are CD silent in the same region. As the presence of a band in the CD spectrum of this kind of system could be due to a deracemization process, to an induced CD effect (ICD) or to the superimposition of

both phenomena, we proved and measured the deracemization by HPLC on a chiral phase. The enantiomeric excesses (ee) determined by HPLC for the deracemization of **4** in aggregates formed by surfactants **2** and **3**, reported in Tables 1 and 2, respectively, show that the aggregates formed by either **2** or **3** have the capability of deracemizing the biphenylic derivative. The ee measured for the sample investigated by  $^1\text{H}$  NMR (40.0 mM in **2** and 4.0 mM in **4**) demonstrates that the splitting of signals observed by NMR (Fig. 3a) is not due to deracemization, because the different intensity of the signals would imply a much higher deracemization extent. Therefore, the double pattern of signals has to be ascribed to specific interactions of **4** with the isomers of the surfactant.

The values of the ee reported in Tables 1 and 2 indicate that the aggregates formed by **2** have a higher recognition capability with respect to **3**. In both cases, the extent of deracemization depends on the [surfactant]/[**4**] ratio, with higher ee's being observed at higher ratios. The requirement of high [surfactant]/[**4**] ratios for observing a higher ee demonstrates that the deracemization is due to the interaction of the probe with a whole region of the aggregate rather than to the interaction with the functional groups adjacent to the stereogenic center of a single monomer within the aggregate.

### 2.3. Chiral recognition experiments on biphenylic derivative **5**

Due to the pattern substitution<sup>8</sup> on the aromatic system, it was expected that the rotational barrier of biphenylic deriv-

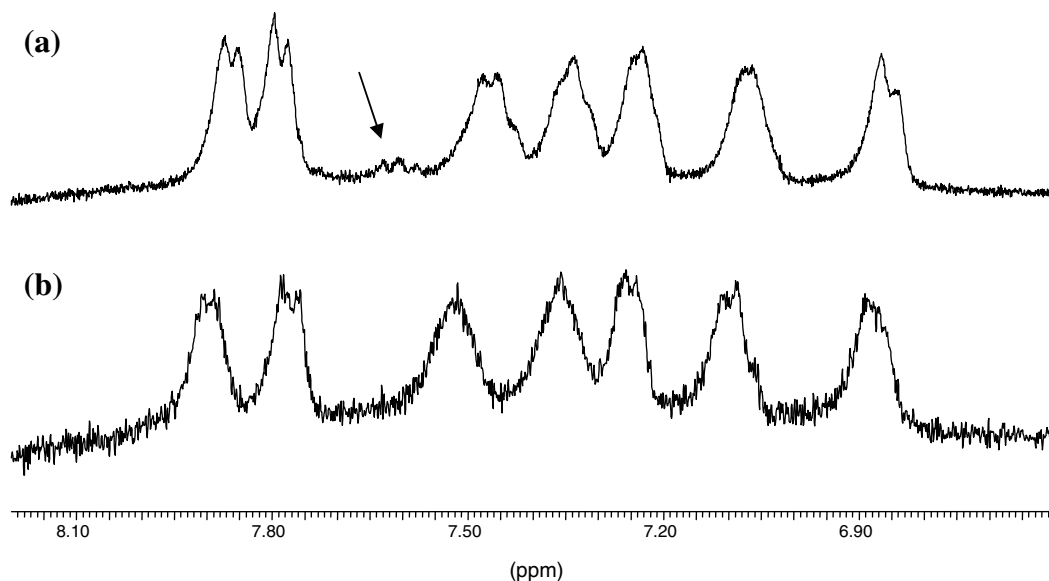


**Figure 3.** Aromatic region of the  $^1\text{H}$  NMR spectrum of 4.0 mM **4** in 40.0 mM aqueous (a) **2**; (b) **3**. The arrow underlines the presence of a signal of lower intensity.

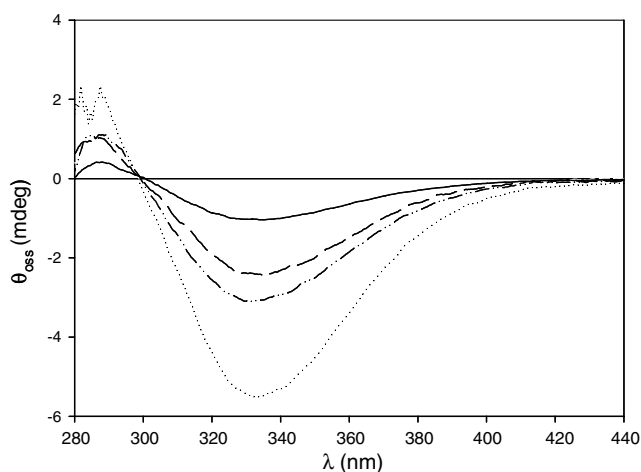


**Figure 4.** CD spectra relative to biphenylic derivative **4** in the presence of aqueous surfactant **2**: 0.4 mM **4** in 40.0 mM **2** (solid line); 0.3 mM **4** in 40.0 mM **2** (dash); 1.0 mM **4** in 100.0 mM **2**, (dash dot dot); 4.0 mM **4** in 40 mM **2**, (dot). Cell path length 0.1 cm.

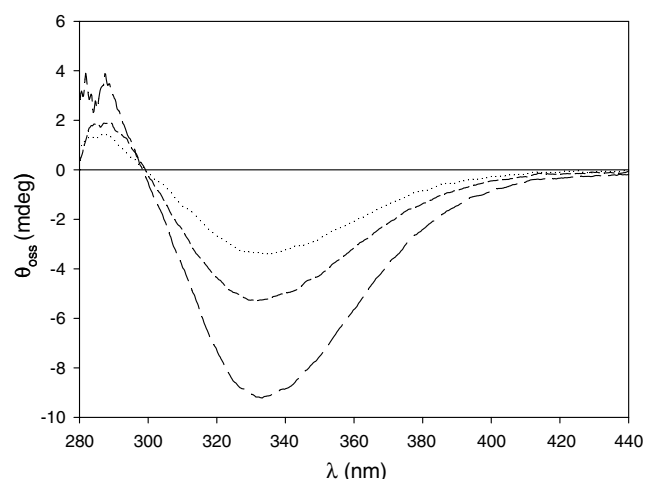


**Figure 5.** CD spectra relative to biphenylic derivative **4** in the presence of aqueous surfactant **3**: 0.4 mM **4** in 40.0 mM **3**, 0.5 cm cell path length (dot); 4.0 mM **4** in 40.0 mM **3**, cell path length 0.1 cm (dash); 1.0 mM **4** in 100 mM **3**, 0.5 cm cell path length (long dash).

ative **5** would be higher with respect to the rotational barrier of **4**; actually, an estimation of the barrier by a theoretical approach gave us a value, in the vacuum, of  $\sim 26$  kcal/mol<sup>3p</sup> that implies a very slow enantiomer interconversion at ambient temperature. However, under the experimental conditions of sample preparation (heating and low power sonication, sample incubation at 303 K prior to measurement), the enantiomer interconversion may become faster while the transfer of the chiral information to the probe should still induce deracemization. In Figure 6, we report the aromatic region of the  $^1\text{H}$  NMR spectra of a 4.0 mM **5** in 40.0 mM aqueous **2** (Fig. 6a) and in 40.0 mM aqueous **3** (Fig. 6b).

Since the  $^1\text{H}$  NMR spectrum reported in Figure 6a shows the presence of two patterns of signals characterized by dif-

ferent intensity, the sample was better investigated at 600 MHz by a 2D COSY experiment, which allowed the assignment of all detectable signals reported in Figure 7. Also, in this case, the split of the signals could be the result of a high extent of deracemization, or it could be due to the

**Table 1.** Enantiomeric excess (ee, %) of **4** resulting from deracemization in aggregates formed by surfactant **2**

[ <b>4</b> ] (mM)	[ <b>2</b> ] (mM)	
	40.0	100.0
0.30	15	
0.40	8	
1.0	6	9
4.0	5	

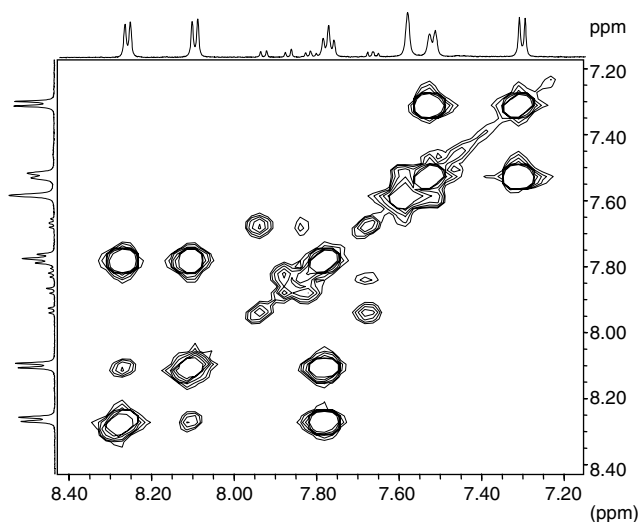
**Table 2.** Enantiomeric excess (ee, %) of **4** resulting from deracemization in aggregates formed by surfactant **3**

[ <b>4</b> ] (mM)	[ <b>3</b> ] (mM)	
	40.0	100.0
0.30	7	
0.40	6	
1.0	5	6
4.0	5	

specific interaction of the biphenylic derivative with the isomers of the surfactant, as observed for probe **4** under the same conditions. The  $^1\text{H}$  NMR spectrum relative to 4.0 mM **5** in 40.0 mM aqueous **3** (Fig. 6b) shows a single pattern of signals.

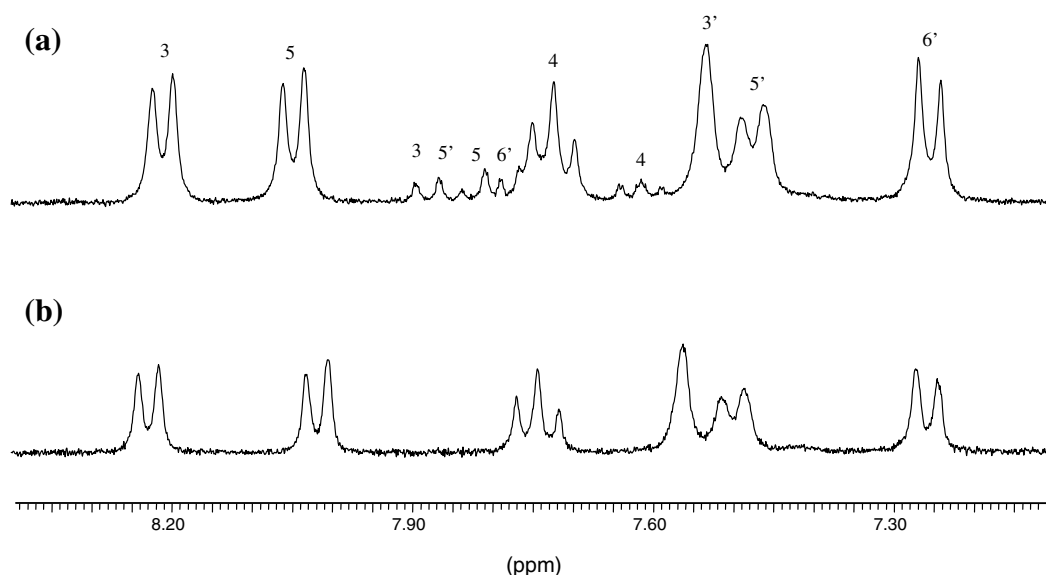
The CD spectrum of 4.0 mM **5** in 40.0 mM aqueous **2** shows a modest bisignate positive curve with maxima at 400 nm and 320 nm (Fig. 8), whereas the corresponding surfactant aqueous solution in the absence of **5** and the corresponding methanol solution containing both **2** and **5** are CD silent in the same region, as well as the aqueous solution of 4.0 mM in **5** and 40.0 mM in **3**.

Since the resolution of the racemic mixture of **5** by HPLC on chiral phases has not been possible in this case, we do not have a definite mean to ascertain and measure the deracemization of **5** in the aggregates formed by surfactant **2**. In fact, in the case of an ICD, the symmetry of the probe is not perturbed, and the CD band is given by the close contact between the host and the guest that allows an efficient coupling between their electric transition moments. However, in an ICD, a bisignate CD curve is observed only if such coupling occurs between two chromophores absorbing in the same or nearly the same region of the spectrum, whereas, if the two interacting systems absorb in different regions, the observed band is not bisignate but has the shape of the guest UV spectrum, positive or negative

**Figure 7.** Aromatic region of the 2D H,H-COSY spectrum of 4.0 mM **5** in aqueous 40.0 mM **2**.

according to the case. Since in our case the interacting transitions are far from the degenerate case, the observed bisignate curve should therefore be due to the interacting aromatic rings of a biphenylic enantiomer, and therefore to a deracemization. A chiral arrangement of the racemic probe should be ruled out because of the lower concentration of probe with respect to the surfactant.

Moreover, because it was reported that the CD curves of acidic solutions of optically active biphenylic derivatives bearing an amino group showed no deflection under the same concentration conditions of the corresponding alkaline solutions,<sup>9</sup> it is reasonable to state that the presence of an ammonium nitrogen on the aromatic ring is responsible for a low molar ellipticity of **5** and, therefore, the observed CD band could be diagnostic of a high extent of deracemization.

**Figure 6.** Aromatic region of the  $^1\text{H}$  NMR spectrum of 4.0 mM **5** in 40.0 mM aqueous (a) **2**; (b) **3**.

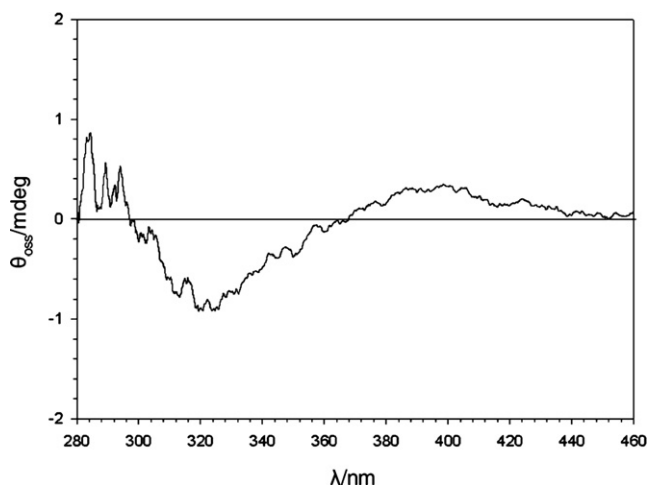


**Figure 8.** CD spectrum of 4.0 mM **5** in the presence of aggregates formed by 40.0 mM **2**. Cell path length is 0.1 cm.

However, it is possible that by NMR and CD we observe different phenomena, the NMR signal split being due to the interaction of **5** with **2** isomers, as observed with biphenylic derivative **4**, and the CD band relative to the same sample revealing the deracemization of **5** inside the aggregates.

In the absence of a definite evidence that could be obtained only after successful separation of the enantiomers, the only thing we can safely claim is that by CD we observe a chiral recognition process.

#### 2.4. $^1\text{H}$ NMR investigation on the micelle binding site of the probes

It is possible to obtain information on the site of binding of the chirality probe, and consequently also on the location of the chiral region(s) of the aggregates through the effect of the aromatic systems of **4** and **5** on the chemical shift of signals due to **2** and **3** in the  $^1\text{H}$  NMR spectra of their aqueous solutions. The chemical shift values, observed in the spectra performed in the absence and in the presence of biphenylic derivative, and the relative differences (all expressed in ppm), are reported in Tables 3 and 4. The values reported in Table 3 show that all signals due to surfactant **2** under aggregating conditions are shifted upfield by the interaction with the aromatic system of **4** with the exception of the resonance due to terminal methyl that is modestly shifted downfield. The most affected resonances by interaction with **4** are those due to the protons in the head-group region ( $\alpha$ ,  $\beta^{anti}$ ,  $\text{N}^+\text{-CH}_3^{anti}$ ,  $2\text{-CH}_2$ ), suggesting a location in the head-group region. In general, the resonances due to **2** are less affected by the interaction with the aromatic system of **5**; moreover, most of the resonances due to head-group protons are downfield shifted, and all other resonances are upfield shifted, with the highest extent of the shift observed for those of the hydrophobic chain, indicating a site of binding in the hydrophobic region of the aggregates. Thus, the results reported in Table 3 suggest a different location of the biphenylic derivatives **4** and **5** in the aggregates formed by **2**. As the chiral recognition experiments performed with both probes gave evidence of the presence of a region capable of chiral recognition, their

**Table 3.** Chemical shift values (ppm) and chemical shift variations (ppm, in brackets) of the resolved  $^1\text{H}$  NMR signals of 40.0 mM surfactant **2** in the absence or the presence of 4.0 mM biphenylic derivatives **4** and **5**

Signal	<b>2</b>	<b>2 + 4</b>	<b>2 + 5</b>
$\alpha_{\text{M}}$	4.406	4.354 (0.052)	4.415 (−0.009)
$\alpha_{\text{m}}$	4.215	4.210 (0.005)	4.221 (−0.006)
$\delta^{anti}$	3.788	3.752 (0.036)	3.786 (0.002)
$\delta^{syn}$	3.723	3.691 (0.032)	3.725 (−0.002)
$\text{N}^+\text{-CH}_3^{syn}$	3.289	3.251 (0.038)	3.293 (−0.004)
$1\text{-CH}_2$	3.228	3.195 (0.033)	3.234 (−0.006)
$\text{N}^+\text{-CH}_3^{anti}$	3.164	3.118 (0.046)	3.164 (0.000)
$\beta^{anti}$	2.559	2.503 (0.053)	2.552 (0.007)
$\beta^{syn}$	2.312	2.290 (0.022)	2.303 (0.009)
$\gamma$	2.312	2.290 (0.022)	2.303 (0.009)
$2\text{-CH}_2$	1.546	1.489 (0.057)	1.537 (0.009)
$3\text{-CH}_2$	1.298	1.278 (0.020)	1.290 (0.008)
Chain	1.268	1.258 (0.010)	1.250 (0.018)
$\omega\text{-CH}_3$	0.851	0.857 (−0.006)	0.838 (0.013)

different sites of binding also suggest the existence of different regions with enantiodiscriminating abilities, that is one close to the head-group region revealed by probe **4**, and another one in the hydrophobic part of the aggregates revealed by probe **5**.

The presence of enantioselective regions in different areas of the aggregates demonstrates that the chiral information is transferred from the monomers to the whole assembly upon aggregation. The chemical shifts and chemical shift differences reported in Table 4 show that also in the aggregates formed by **3** probes **4** and **5** feature different sites of association. Biphenylic derivative **4** is bound close to the head groups in a more restricted region with respect to its position in the **2** aggregates, as demonstrated by the downfield shift of resonances due to  $\delta$  protons and alkyl chain protons, whereas biphenylic derivative **5** is located in the hydrophobic region of the aggregate, as suggested by the high extent of upfield shift of the resonance due to the alkyl chain protons. In the aggregates formed by **3**, we have evidence of chiral recognition only in the experiment performed with biphenylic derivative **4**, that is in correspondence of a site of binding close to the head-group region, thus in these aggregates we marked a chiral region only in the head-group area.

The subtle variation in the structure of the amidic surfactants strongly influences the organization of their aggregates, and the transfer and expression of the chiral information.



**Table 4.** Chemical shift values (ppm) and chemical shift variations (ppm, in brackets) of the resolved  $^1\text{H}$  NMR signals of 40.0 mM surfactant **3** in the absence and in the presence of 4.0 mM biphenylic derivatives **4** and **5**

Signal	<b>3</b>	<b>3 + 4</b>	<b>3 + 5</b>
$\alpha_{\text{m}}$	4.944	4.955 (−0.011)	4.985 (−0.041)
$\alpha_{\text{M}}$	4.876	4.875 (0.001)	4.900 (−0.024)
$\delta$	3.860	3.875 (−0.015)	3.861 (−0.001)
$\delta$	3.690	3.710 (−0.020)	3.716 (−0.026)
1-CH <sub>2</sub>	3.498	3.485 (0.013)	3.500 (−0.002)
N <sup>+</sup> -CH <sub>3m</sub>	3.282	3.281 (0.001)	3.308 (−0.026)
1-CH <sub>2</sub>	3.263	3.256 (0.007)	3.260 (0.003)
N <sup>+</sup> -CH <sub>3</sub> <sup>anti</sup>	3.256	3.252 (0.004)	3.276 (−0.020)
N <sup>+</sup> -CH <sub>3</sub> <sup>syn</sup>	3.248	3.238 (0.010)	3.263 (−0.015)
N <sup>+</sup> -CH <sub>3m</sub>	3.187	3.184 (0.003)	3.204 (−0.017)
N-CH <sub>3</sub>	3.156	3.135 (0.021)	3.166 (−0.010)
N-CH <sub>3m</sub>	2.947	2.298 (0.019)	2.948 (−0.001)
$\beta^{\text{anti}}$	2.665	2.661 (0.004)	2.665 (0.000)
$\gamma$	2.336	2.320 (0.016)	2.329 (0.007)
$\beta^{\text{syn}}$	2.184	2.181 (0.003)	2.180 (0.004)
2-CH <sub>2</sub>	1.528	1.518 (0.010)	1.527 (0.001)
3-CH <sub>2</sub>	1.293	1.288 (0.005)	1.215 (0.078)
Chain	1.262	1.270 (−0.008)	1.261 (0.001)
$\omega$ -CH <sub>3</sub>	0.852	0.864 (−0.012)	0.851 (0.001)

### 3. Conclusions

The chiral recognition capabilities of aggregates formed by chiral cationic surfactants were explored by using two biphenylic derivatives as probes of chirality. Subtle changes of the molecular structure of the surfactant influence their aggregating properties and their recognition capabilities. Chiral recognition processes occur in different regions of the aggregates, also in sites remote from the stereogenic centers, where recognition cannot be observed at the monomer level, thus demonstrating that the aggregation process translates the recognition capability to the whole aggregate.

### 4. Experimental

#### 4.1. Materials

Chemicals (Sigma–Aldrich) were of the highest grade available and used without further purification. Solvents

employed in the spectroscopic studies were of spectroscopic grade and used as received.

#### 4.2. Instrumentation

$^1\text{H}$  and  $^{13}\text{C}$  NMR spectra were recorded on a Bruker AC 300 operating at 300.13 and 75.47 MHz for  $^1\text{H}$  and  $^{13}\text{C}$ , respectively, equipped with a sample tube thermostating apparatus. The 2D H,H-COSY spectrum was recorded on a Bruker AVANCE AQS600 operating at 600.13 MHz. Signals were referenced with respect to TMS ( $\delta = 0.000$  ppm), used as internal standard in CD<sub>3</sub>OD, and to DOH ( $\delta = 4.75$  ppm at 298 K) in D<sub>2</sub>O.

Fluorescence nanosecond decays were measured by a CD900, SPC lifetime apparatus from Edinburgh Instruments. Excitation was achieved by an arc flashlamp filled by ultrapure hydrogen (300 mmHg; FWHM (full-width half maximum) = 1.2 ns at 30 kHz repetition rate);  $I_{\text{ex}} = 325$  nm,  $I_{\text{em}} = 395$  nm. Experimental decay curves were fitted by non-linear least-squares analysis to exponential function through an iterative reconvolution procedure. The decay of a fluorescent probe in the presence of a quencher in a micelle was accounted for by the equation:<sup>4</sup>

$$I(t) = I(0) \exp\{-t/\tau_0 - C[1 - \exp(-k_q t)]\}$$

where  $\tau_0$  is the time decay of the probe (measured separately in the same experimental conditions, but in the absence of the quencher),  $k_q$  is the quenching rate constant, and  $C$  is the average number of quenchers per micelle. The aggregation number is then obtained by the equation:<sup>4a</sup>

$$N = ([D] - \text{cmc})C/[\text{CPyC}]$$

where  $[D]$  is the molar concentration of surfactant,  $[\text{CPyC}]$  is the molar concentration of cetylpyridinium chloride, and cmc is the critical micellar concentration.

Conductivity measurements were carried out at 298 K on a Hanna conductimeter HI-9932, equipped with a thermostating apparatus. CD spectra were recorded on a Jasco spectropolarimeter J-715. HPLC determinations of enantiomeric excess were performed as previously described.<sup>7a,b</sup>

#### 4.3. Preparation of biphenylic derivatives and surfactants

Biphenylic derivatives were prepared as previously reported.<sup>3p</sup>

**4.3.1. (2S)-N-Dodecyl-1,1-dimethylpyrrolidinium-2-carboxamide bromide 2.** A solution of 1.2 g (3.4 mmol) of *N*-dodecyl-1-methylpyrrolidine-2-carboxamide in 16 mL of methanol was saturated with CH<sub>3</sub>Br and left under a CH<sub>3</sub>Br atmosphere and under stirring until complete disappearance of the starting material (~4 days, TLC: CH<sub>3</sub>OH/Et<sub>2</sub>O 95/5). The solvent was then removed under vacuum and the residue was washed several times with Et<sub>2</sub>O in order to obtain the desired product in 91% yield. Mp 361–363 °C.  $^1\text{H}$  NMR,  $\delta$  (CD<sub>3</sub>OD): 0.971 (t, 12-CH<sub>3</sub>, 3H); 1.364 (m, C<sub>3</sub>–C<sub>11</sub>, 18H); 1.633 (m, 2-CH<sub>2</sub>, 2H); 2.392 (m, H <sub>$\beta$</sub> , 2H <sub>$\gamma$</sub> , 3H); 2.630 (m, H <sub>$\beta$</sub> , 1H); 3.270 (s, N<sup>+</sup>-

CH<sub>3</sub>, 3H); 3.320 (t, 1-CH<sub>2</sub>, 2H); 3.394 (s, N<sup>+</sup>-CH<sub>3</sub>, 3H); 3.797 (m, H<sub>δ</sub>, 1H); 3.917 (m, H<sub>δ</sub>, 1H); 4.410 ppm (t, H<sub>α</sub>, 1H). <sup>13</sup>C NMR, δ (CD<sub>3</sub>OD): 14.78 (C12); 21.53 (Cγ); 24.02 (C11); 28.32 (C3); 26.98 (Cβ); 30.34 (C2); 30.64 (C9); 30.75–31.03 (C4, C5, C6, C7, C8); 33.34 (C10); 41.07 (C1); 48.07 (N<sup>+</sup>-CH<sub>3</sub>); 53.71 (N<sup>+</sup>-CH<sub>3</sub>); 68.15 (Cδ); 76.04 (Cα); 166.92 ppm (CO). [α]<sub>D</sub> = −12.6 (c 2.125, MeOH).

**4.3.2. (2S)-N-Dodecyl-1-methylpyrrolidine-2-carboxamide.** 1-Hydroxybenzotriazole (HOBt) (477 mg, 3.5 mmol) and 677 mg (4 mmol) of *N*-(3-dimethylaminopropyl)-*N'*-ethylcarbodiimide hydrochloride (EDC-HCl) were added, at 298 K, under stirring, to a solution of 520 mg (4.0 mmol) of *N*-methyl-L-proline in 25 mL of anhydrous CH<sub>2</sub>Cl<sub>2</sub>. The mixture was kept at 298 K for 1 h, then 1.3 g (7.1 mmol) of 1-aminododecane was added and the mixture was allowed to warm to room temperature. After completion of the reaction (~24 h), the solvent was removed under reduced pressure and the residue solubilized in Et<sub>2</sub>O. The organic solution was washed with a saturated NaHCO<sub>3</sub> aqueous solution, with brine and finally dried over Na<sub>2</sub>SO<sub>4</sub>. Purification by chromatography on silica gel (CH<sub>3</sub>OH/Et<sub>2</sub>O = 95/5) of the residue obtained after filtration of the solution and removal of the solvent under vacuum yielded the pure product, a yellow oil, in a 54% yield. <sup>1</sup>H NMR, δ (CD<sub>3</sub>OD): 0.859 (t, 12-CH<sub>3</sub>, 3H); 1.235 (m, C<sub>3</sub>–C<sub>11</sub>, 18H); 1.480 (m, 2-CH<sub>2</sub>, 2H); 1.742 (m, H<sub>β</sub>, 2H<sub>γ</sub>, 3H); 2.200 (m, H<sub>β</sub>, 1H); 2.333 (m, N-CH<sub>3</sub>, H<sub>δ</sub>, 4H); 2.838 (q, H<sub>α</sub>, 1H); 3.066 (m, H<sub>δ</sub>, 1H); 3.218 ppm (m, 1-CH<sub>2</sub>, 2H). <sup>13</sup>C NMR, δ (CD<sub>3</sub>OD): 14.58 (C12), 23.72 (C11), 24.75 (Cγ), 27.92 (C3), 30.39 (C9), 30.47 (C8), 30.55 (C2), 30.69–30.77 (C7, C6, C5, C4), 31.75 (Cβ), 32.10 (C10), 39.86 (C1), 41.64 (N-CH<sub>3</sub>), 57.40 (Cδ), 70.12 (Cα), 176.33 ppm (CO).

*N*-Methyl-L-proline was prepared as previously described.<sup>10</sup>

(2S)-*N*-Dodecyl-*N*,1,1-trimethylpyrrolidinium-2-carboxamide bromide, **3**, was prepared in 90% yield from *N*-dodecyl-*N*,1-dimethylpyrrolidine-2-carboxamide following the same procedure used to prepare surfactant **2**. Mp 339–341 K. <sup>1</sup>H NMR, δ (CDCl<sub>3</sub>): 0.829 (t, 12-CH<sub>3</sub>, 3H); 1.204 (m, C<sub>3</sub>–C<sub>11</sub>, 18H); 1.463 (m, 2-CH<sub>2</sub>, 2H); 2.036 (m, H<sub>β</sub>, 1H); 2.141 (m, H<sub>γ</sub>, 1H); 2.375 (m, H<sub>γ</sub>, 1H); 2.595 (m, H<sub>β</sub>, 1H); 2.903–3.235 (d, N-CH<sub>3</sub>, 3H); 3.150–3.450 (1-CH<sub>2</sub>, 2H); 3.342–3.370 (d, N<sup>+</sup>-CH<sub>3</sub><sup>anti</sup>, 3H); 3.547–3.569 (d, N<sup>+</sup>-CH<sub>3</sub><sup>syn</sup>, 3H); 3.927 (m, H<sub>δ</sub><sup>anti</sup>, 1H); 4.221 (m, H<sub>δ</sub><sup>syn</sup>, 1H); 5.638–5.744 ppm (t, H<sub>α</sub>, 1H). <sup>13</sup>C NMR, δ (CDCl<sub>3</sub>): 13.92 (C12); 20.11 (Cγ, Z); 20.30 (Cγ, E); 22.47 (C11); 25.50–26.33 (Cβ); 26.39 (C3); 26.60 (C9); 26.70–28.91 (C2); 29.07–29.40 (C4, C5, C6, C7, C8), 31.06 (C10); 34.04–36.35 (N-CH<sub>3</sub>); 47.64–47.90 (N<sup>+</sup>-CH<sub>3</sub><sup>anti</sup>); 51.76 (N<sup>+</sup>-CH<sub>3</sub><sup>syn</sup>); 48.50–50.45 (C1); 66.19–66.27 (Cδ); 70.18–70.61 (Cα); 165.47–165.58 (CO) ppm. [α]<sub>D</sub> = −27.3 (c 1.75, MeOH).

(2S)-*N*-Dodecyl-*N*,1-dimethylpyrrolidine-2-carboxamide (a yellow oil) was obtained in a 59% yield from *N*-methyl-L-proline and *N*-methyl-1-aminododecane. <sup>1</sup>H NMR, δ (CDCl<sub>3</sub>): 0.867 (t, 12-CH<sub>3</sub>, 3H); 1.230 (m, C<sub>3</sub>–C<sub>11</sub>, 18H); 1.520 (m, 2-CH<sub>2</sub>, 2H); 1.700–2.180 (m, 2H<sub>β</sub>, 2H<sub>γ</sub>, 4H); 2.240 (q, H<sub>δ</sub>, 1H); 2.316 (d, N-CH<sub>3</sub>, 5H); 2.913–3.053 (s,

C(O)N-CH<sub>3</sub>, 3H); 3.075 (t, H<sub>α</sub>, 1H); 3.100 (m, H<sub>δ</sub>, 1H); 3.362 ppm (m, 1-CH<sub>2</sub>, 2H). <sup>13</sup>C NMR, δ (CDCl<sub>3</sub>): 14.16 (C12), 22.73 (C11), 23.05–23.14 (Cγ), 26.80 (C3), 27.17–28.87 (C2), 29.10 (Cβ), 29.39–29.82 (C9, C8, C7, C6, C5, C4, Cβ), 31.96 (C10), 33.83–34.77 (C(O)N-CH<sub>3</sub>), 40.73 (N-CH<sub>3</sub>), 48.07–49.39 (C1), 56.19 (Cδ), 66.09–66.60 (Cα), 171.72–172.28 ppm (CO).

#### 4.4. Samples preparation

Samples of 4.0 mM biphenylic derivative in 40.0 mM aqueous surfactant were prepared by adding to the proper amounts of surfactant and biphenylic derivative 0.700 mL of D<sub>2</sub>O. The solutions were sonicated and gently heated to obtain clear solutions.

Samples at a lower concentration of biphenylic derivative were prepared following the ethanol injection method, adding a proper volume of a concentrated ethanol solution of biphenylic derivative to the aqueous solution of surfactant. All samples were incubated at 303 K overnight prior to measurement.

#### 4.5. Determination of cmc of surfactants **2** and **3**

Critical micellar concentration of surfactants **2** and **3** was determined by conductivity measurements of solutions obtained by adding known volumes of 50 mM aqueous solution of surfactant to a known volume of bidistilled water.

#### 4.6. Determination of the aggregation number of surfactants **2** and **3**

Fluorescence experiments were carried out on aqueous solutions 40 and 100 mM in surfactant **2** or **3**, 0.50 mM in CPyCl, 5.2 μM in Pyrene. In diluting stock solutions, the ratio [surfactant]/[quencher]/[fluorophore] was kept constant in order to have a Poissonian distribution of the quencher among the micelles. Aggregation numbers were reproducible within 5%.

#### Acknowledgments

This work has been carried out in the frame of the project 'The use of surfaces and vesicles for the amplification of homochirality in polypeptide chains' of COST action D27. We acknowledge contributions from CNR, Dipartimento di Progettazione Molecolare. C.V. and S.L.M. acknowledge fundings from PRIN Contract No. 2005037725.

#### References

- (a) Zanasi, R.; Lazzaretti, P.; Ligabue, A.; Soncini, A. *Phys. Rev. E* **1999**, *59*, 3382–3385; (b) Lazzaretti, P.; Zanasi, R.; Faglioni, F. *Phys. Rev. E* **1999**, *60*, 871–874; (c) Berger, R.; Quack, M. *ChemPhysChem* **2000**, *1*, 57–60; (d) Johnson, L. N. *Euro. Rev.* **2005**, *13*, 77–95; (e) Fitz, D.; Reiner, H.; Plankenstein, K.; Rode, B. M. *Curr. Chem. Biol.* **2007**, *1*, 41–52.



2. (a) Laursen, R. A.; Wen, D.; Knight, C. A. *J. Am. Chem. Soc.* **1994**, *116*, 12057–12058; (b) Orme, C. A.; Noy, A.; Wierzbicki, A.; McBride, M. T.; Grantham, M.; Teng, H. H.; Dove, P. M.; De Yoreo, J. J. *Nature* **2001**, *411*, 775–779; (c) De Feyter, S.; Gesquière, A.; Wurst, K.; Amabilino, D. B.; Veciana, J.; De Schryver, F. C. *Angew. Chem.* **2001**, *113*, 3317–3320; (d) Ribo, J. M.; Crusats, J.; Sagués, F.; Claret, J.; Rubires, R. *Science* **2001**, *292*, 2063–2066; (e) Zepik, H.; Shavit, E.; Tang, M.; Jensen, T. R.; Kjaer, K.; Bolbach, G.; Leiserowitz, L.; Weissbuch, I.; Lahav, M. *Science* **2002**, *295*, 1266–1269; (f) Geva, M.; Frolow, F.; Eisenstein, M.; Addadi, L. *J. Am. Chem. Soc.* **2003**, *125*, 696–704; (g) Levy-Lior, A.; Weiner, S.; Addadi, L. *Helv. Chim. Acta* **2003**, *86*, 4007–4017; (h) Purrello, R. *Nat. Mater.* **2003**, *2*, 216–217; (i) Crusats, J.; Claret, J.; Diez-Perez, I.; El-Hachemi, Z.; García-Ortega, H.; Rubires, R.; Sagués, F.; Ribo, J. M. *J. Chem. Soc., Chem. Commun.* **2003**, 1588–1589; (j) Mateos-Timoneda, M. A.; Crego-Calama, M.; Reinhoudt, D. N. *Chem. Soc. Rev.* **2004**, *33*, 363–372.
3. (a) Arnett, E. M.; Gold, J. M. *J. Am. Chem. Soc.* **1982**, *104*, 636–639; (b) Fuhrop, J. H.; Schnieder, P.; Rosenberg, J.; Boekema, E. *J. Am. Chem. Soc.* **1987**, *109*, 3387–3390; (c) Morigaki, K.; Dallavalle, S.; Walde, P.; Colonna, S.; Luisi, P. L. *J. Am. Chem. Soc.* **1997**, *119*, 292–301; (d) Walde, P.; Blöchliger, E. *Langmuir* **1997**, *13*, 1668–1671; (e) Bella, J.; Borocci, S.; Mancini, G. *Langmuir* **1999**, *15*, 8025–8031; (f) Uragami, M.; Miyake, Y.; Regen, S. L. *Langmuir* **2000**, *16*, 3491–3496; (g) Lalitha, S.; Kumar, A. S.; Stine, K. J.; Covey, D. F. *J. Supramol. Chem.* **2001**, *1*, 53–61; (h) Borocci, S.; Ceccacci, F.; Galantini, L.; Mancini, G.; Monti, D.; Scipioni, A.; Venanzi, M. *Chirality* **2003**, *15*, 441–447; (i) Bombelli, C.; Borocci, S.; Lupi, F.; Mancini, G.; Mannina, L.; Segre, A. L.; Viel, S. *J. Am. Chem. Soc.* **2004**, *126*, 13354–13362; (j) Nakagawa, H.; Yoshida, M.; Kobori, Yuuki; Yamada, K.-I. *Chirality* **2003**, *15*, 703–708; (k) Addona, G. H.; Sandermann, H., Jr.; Kloczewiak, M. A.; Miller, K. W. *Biochim. Biophys. Acta* **2003**, *1609*, 177–182; (l) Andreani, R.; Bombelli, C.; Borocci, S.; Lah, J.; Mancini, G.; Mencarelli, P.; Vesnaver, G.; Villani, C. *Tetrahedron: Asymmetry* **2004**, *15*, 987–994; (m) Suchyna, T. M.; Tape, S. E.; Koeppe, R. E., II; Andersen, O. S.; Sachs, F.; Gottlieb, P. A. *Nature* **2004**, *430*, 235–240; (n) Epand, R. M.; Rychnovsky, S. D.; Belani, J. D.; Epand, R. F. *Biochem. J.* **2005**, *390*, 541–548; (o) Nakagawa, H.; Onoda, M.; Masuoka, Y.; Yamada, K.-I. *Chirality* **2006**, *18*, 212–216; (p) Ceccacci, F.; Giansanti, L.; Mancini, G.; Mencarelli, P.; Sorrenti, A. *New J. Chem.* **2007**, *31*, 86–92.
4. (a) Alargova, R. G.; Kochijashky, I. I.; Sierra, M. L.; Zana, R. *Langmuir* **1998**, *14*, 5412–5418; (b) Hansson, P.; Jönsson, B.; Ström, C.; Söderman, O. *J. Phys. Chem.* **2000**, *104*, 3496–3506.
5. (a) Cerichelli, G.; Luchetti, L.; Mancini, G. *Langmuir* **1997**, *13*, 4767–4769; (b) Borocci, S.; Mancini, G.; Cerichelli, G.; Luchetti, L. *Langmuir* **1999**, *15*, 2627–2630.
6. Tobler, E.; Lämmerhofer, M.; Mancini, G.; Lindner, W. *Chirality* **2001**, *13*, 641–647.
7. (a) Ceccacci, F.; Diociaiuti, M.; Galantini, L.; Mancini, G.; Mencarelli, P.; Scipioni, A.; Villani, C. *Org. Lett.* **2004**, *6*, 1565–1568; (b) Ceccacci, F.; Mancini, G.; Sferrazza, A.; Villani, C. *J. Am. Chem. Soc.* **2005**, *127*, 13762–13763.
8. Wolf, C.; König, W. A.; Roussel, C. *Liebigs Ann.* **1995**, 781–786.
9. Mislow, K.; Bunnenberg, E.; Records, R.; Wellman, K.; Djerassi, C. *J. Am. Chem. Soc.* **1963**, *85*, 1342–1349.
10. Möhrle, Sieker. *ARPMAS, Arch. Pharm. (Weinheim Ger)* **1976**, *309*, 380–382.